Journal of Molecular Catalysis B: Enzymatic 69 (2011) 133–139

Contents lists available at ScienceDirect

Journal of Molecular Catalysis B: Enzymatic

journal homepage: www.elsevier.com/locate/molcatb

Biocatalytic microreactor incorporating HRP anchored on micro-/nano-lithographic patterns for flow oxidation of phenols

Madalina Tudorache[a], Diana Mahalu[b], Cristian Teodorescu[c], Razvan Stan[d], Camelia Bala[e,*], Vasile I. Parvulescu[a,*]

[a] University of Bucharest, Department of Chemical Technology and Catalysis, Bd. Regina Elisabeta 4-12, Bucharest 030016, Romania
[b] Braun Center for Submicron Research, Department of Condensed Matter Physics, Weizmann Institute of Science, PO Box 26, Rehovot 76100, Israel
[c] National Institute of Materials Physics, Atomistilor Str. 105bis, PO Box MG 7, Magurele-Bucharest 077125, Romania
[d] Huygens Laboratory, Biophysics Dept., Leiden University, PO Box 9500, 2300 RA Leiden, The Netherlands
[e] University of Bucharest, Department of Analytical Chemistry, Bd. Regina Elisabeta 4-12, Bucharest 030016, Romania

ARTICLE INFO

Article history:
Received 8 September 2010
Received in revised form
15 December 2010
Accepted 19 January 2011
Available online 26 January 2011

Keywords:
Biocatalytic microreactor
Micro-/nano-pattern
Horseradish peroxidase (HRP)
Bio-oxidation
Phenolic compounds

ABSTRACT

A highly durable and versatile micro scale biocatalytic reactor has been designed and investigated in the heterogeneous enzyme-catalytic oxidation of phenols. It consisted of optical or electron beam lithographic gold deposited layer with different thickness from nano- to micro-scale on a semiconductor surface. Horseradish peroxidase (HRP) enzyme was immobilized on the gold-surface using two different approaches (i.e., physical adsorption and self-assembled monolayer). Characterization of those HRP-gold surfaces was made using AFM (atomic force microscopy) coupled with ellipsometry measurements, SEM (scanning electron microscopy), STM (scanning tunneling microscopy) and spectrophotometric technique. The catalytic performances of the developed structures were investigated after their incorporation in microreactors using a recycling-flow system dedicated to phenols oxidation. In order to optimize the efficiency of the oxidation process it was checked the effect of the successively addition of the reagent, the influence of the reaction time, the stability and the reuse of the biocatalytic micro-system. Maximum phenol conversion was of 35.1%. In addition to phenol the system has also been investigated in oxidation of other phenolic compounds such as cathecol, hydroquinone, rezorcine, β-naphtol, o/p-aminophenol and 4-metoxyphenol.

1. Introduction

The concept of reactor miniaturization, novel technology of nowadays for successful scale-up of catalytic and biocatalytic processes represent promising tool to replace batch technological based and conventional-scale reactors in a more effective way [1–3]. Various aspects of technological and biotechnological processes such as on-site and on-demand production of hazardous chemicals, requirement of an integral component within the framework of process miniaturization as well as a means of process intensification [4–6] support this concept. Advantages include improvement in surface to volume ratio, large interfacial area allowing multiphase reaction systems, efficient mass transfer leading to a shorter diffusion time of the reagent to the active sites of the catalyst, enhancement of the reaction kinetics, low consumption of reagents, sample and energy [7,8].

Phenols biocatalytic oxidation in the presence of peroxidase as biocatalyst is still one of the most useful reaction in the area of phenol-industry. The current view of process mechanism entails the direct one electron oxidation of phenols molecule in the presence of hydrogen peroxide followed by coupling of the resulted radicals with the formation of a wide array of polymeric products that precipitate from the solution [9]. Bio-oxidation of phenol furnishes more hydroxylated aromatic compounds that can be oxidized to quinones while further oxidation give a complex mixture of organic compounds with high content of polyphenols [10]. Enzymatic synthesis of polyphenols has the advantages of high catalytic activity, mild reaction conditions, high regioselectivity and the absence of by-product formation [11]. Thus, peroxidase enzymes have been reported to catalyse phenolic polymers and copolymers synthesis from a wide range of phenols, including p-cresol, p-phenylphenol, various naphtols, and phenol itself, along with related anilines [12–16]. In particular, horseradish peroxide (HRP) has demonstrate a great ability to catalyse the oxidation of phenols followed by polymerization of oxidized phenols in homogeneous and also heterogeneous forms [17,18].

HRP enzyme can be advantageously used in immobilized form turns the enzyme-based phenol oxidation into a more

* Corresponding authors. Tel.: +40 21 4100241; fax: +40 21 4100241.
E-mail addresses: camelia.bala@g.unibuc.ro (C. Bala), vasile.parvulescu@g.unibuc.ro (V.I. Parvulescu).

1381-1177/$ – see front matter © 2011 Elsevier B.V. All rights reserved.
doi:10.1016/j.molcatb.2011.01.007

economically viable approach. As an important advantage the immobilized enzyme (e.g. HRP) is frequently more stable towards harsh experimental conditions such as higher temperatures or different pH [19]. Thus, the biocatalyst can survive longer during the process conditions and can also be reused several times. Packed bed reactors have been used for this purpose. The HRP immobilization was carried out on glass beads, polymers, filter paper, nylon balls, etc. [20–22]. The enzyme was supported using different immobilization procedures which had a direct influence on the preservation of the HRP activity, such as physical adsorption, cross-linking, entrapment, bioaffinity coupling and covalent attachment (providing a better orientation of the biocatalyst on the reactor surface) [20,23–25]. In covalent immobilization, selective activation and coupling procedures have been performed for support pretreatment leading to epoxy-, carboxylic- or amino-activated support allowing enzyme coupling [26–29]. HRP-reactors have been designed as disk, bed or tubular reactor specifically for batch, semi-bach and continuous flow (e.g. simple continuous, combined continuous-–stopped or recycling continuous flow) systems [30–32]. In a slurry reactor, homogeneous polymerization is enhanced in the bulk liquid phase while it is suppressed in a liquid-full operated fixed bed reactor due to the high solid to liquid ratio [33,34]. Miniaturization of HRP-microreactor is another important target with significant contributions to cost reduction and efficiency improvement as well as giving a "greener direction" to the process. However, this topic is still under investigations [35–38].

In this paper a HRP-microreactor with micro-/nano-gold pattern deposed on silicon holders by optical or electronic lithography is described and characterized based on its catalytic properties on phenols oxidation process. The HRP enzyme is adsorbed or covalently immobilized on the gold pattern surface testing the approach advantages for increased volumetric productivity and improved stability. The miniaturized biocatalytic reactor was of a tubular type and was evaluated under recycling-flow conditions.

2. Experimental

2.1. Chemicals and instruments

Phosphate buffer saline (PBS) was prepared as stock solution of 100 mM concentration according to the following method: 80 g NaCl, 2 g KCl, 14.3 g $Na_2HPO_4{\cdot}2H_2O$ and 3.43 g KH_2PO_4 were dissolved in 1 l distilled water and the pH was adjusted with either NaOH or HCl.

Stock solution of phenol (10 mM) was prepared in 10 mM PBS solution (pH 7.4). Also, the enzyme (HRP-Peroxidase from horseradish, Sigma Type VI, product number P8375-25 KU, lot number 097K7675, 259 U/mg) was dissolved in PBS (100 mM, pH 7.4) in order to obtain a solution of 250 units/mL concentration for bioreactor preparation. H_2O_2 stock solution (33%) was daily diluted in phenol solution (10 mM) until 1 M H_2O_2 concentration since fresh solution needed to be used for the experiments. 11-mercapto-undecanoic acid thiol (11-MUA 95%), 1-ethyl-3-(3-dimethylamino-propyl)-carbodiimide hydrochloride (EDC) and N-hydroxysuccinimide ester (NHS) were used as immobilization reagents for HRP attachment on the gold surface of the bioreactor. All the solution reagents and chemicals were purchased from Sigma–Aldrich and Merck.

HPLC-UV/Vis (Thermo Scientific ACCELA) system was used for analytic measurements. The system was equipped with a RP C18 column and UV–VIS detector. The measurements were carried out under the following experimental conditions: 1 mL/min flow rate of the mobile phase (85% solution 0.5% acetic acid and 15% methanol) and 254 nm wavelength of the UV–VIS detector. ^{1}H- and ^{13}C-MAS NMR spectra were recorded at room temperature on MAS-NMR Avance 400 Bruker spectrometer, at 400 (^{1}H) and 100.5 (^{13}C) MHz, in a 9.4 T field, with 15 kHz spinning rate. Deconvolution of the CP/MAS NMR spectra was carried out using the DMFIT program [39].

2.2. Preparation of the micro-patterns and nano-patterns

Micro-patterns were prepared with features bigger than 1 μm and "zig-zag" design on silicon wafers (pieces of length × width = 10 mm × 6 mm). They were inserted in the reactor walls. These samples were coated with photo-resist on silicon wafers (standard 5.08 cm P100 (p type, orientation 100) silicon wafer). The process was based on the image reversal technique for "bight field" contact masks. Standard contact optical lithography, using a 10.16 cm Karl–Suss mask-aligner, was followed by developing and lift-off, as before. Note that 1 μm features are a comfortable resolution limit for contact optical lithography when using a 405 nm wavelength exposure (the rule of thumb being that one can easily expose patterns with a typical size bigger than 2λ). The optical lithography was followed by metal lift-off technique, as before.

For nano-patterns a linear design was used with typical dimensions smaller than 0.3 μm. The samples were exposed on a double layer of polymethylmethacrylate resist spin-coated on silicon wafers (standard 5.08 cm P100 (p type, orientation 100) silicon wafer). The exposure was done by direct write electron beam lithography (using a 100 kV JEOL JBX-9300 machine), followed by one minute development in methyl-isobuthyl ketone: isopropanol = 1:3 solution. The desired gold metal layer was deposited over the entire wafer using an electron gun evaporator in high vacuum (10^{-6} Torr). Note that, previous to gold evaporation, a thin titanium layer (~10 nm) was added in order to insure gold adhesion on silicon. Finally, the desired pattern is obtained by lift-off technique using hot acetone and isopropanol for rinse. In both cases, the metal thickness was measured using a Dektak 6M stylus profilometer, while samples characterization was done by SEM (scanning electron microscopy) analysis (SEM Zeiss Supra 55).

2.3. Characterization of the micro-/nano-patterns

Atomic force microscopy (AFM) coupled with ellipsometry measurements were carried out with a Tapping Mode AFM equipped with a Digital Instruments Nanoscope IIIa controller. Tips were purchased from Olympus and had a nominal value of the spring constant of 2 N/m. Images were acquired in air. Scanning tunneling microscopy (STM) was performed using a variable temperature Aarhus system (Specs, Germany) operating in 10^{-9} mbar vacuum range using a tungsten tip. The tunneling current was in the range 1–10 nA. Pictures were collected for surfaces of 20 A × 20 A.

2.4. HRP immobilization on gold patterns

The immobilization of the HRP enzyme on the gold patterns was performed using the physical adsorption and self-assembled monolayer methods. In both cases, the procedure was launched with a washing step when the reactor surface was flushed with acidic solution (93–95% H_2SO_4) and dried with pure acetone. Physical adsorption of the enzyme on the reactor surface (microreactor M_1) was performed by a simple addition of the enzyme solution (100 μL of HRP solution 250 units/mL) on the reactor surface and then left in the contact for 2 h at room temperature. At the end, the reactor surface was gently washed with PBS solution (100 mM, pH 7.4).

In the self-assembled monolayer procedure the reactor surface was pre-treated with a solution of thiol followed by covalent

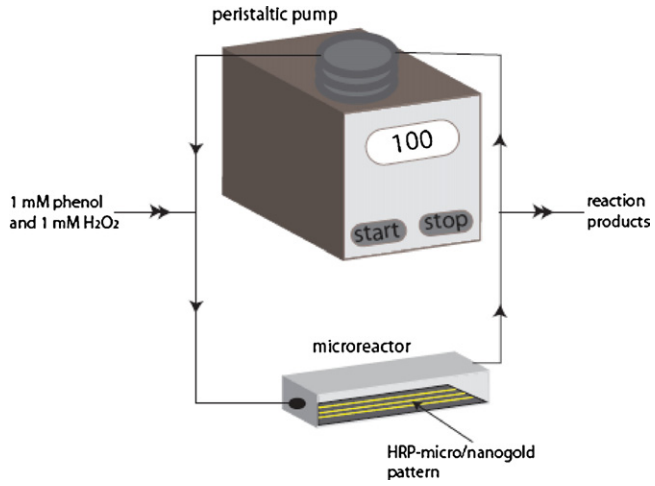

Fig. 1. Recycling flow micro-system for biocatalytic oxidation of phenols.

immobilization of the HRP enzyme (100 μL of HRP solution 250 units/mL) through the disposable $-NH_2$ groups of the enzyme and –COOH end-groups of the thiol chain. Therefore, the reactor was immersed in a thiol solution (10 mg mL^{-1} of 11-MUA) immediately after the washing step. The contact time between the reactor gold surface and the thiol solution was of 2 h (at room temperature). Then, the reactor surface was washed with ethanol and dried to remove the excess of thiol. In the next step, the –COOH terminal groups of the thiol chain were activated by immersing the reactor in 1 mL solution 50 mM NHS and 200 mM EDC. The activation time was of 2 h. The addition of the enzyme solution to the reactor surface represented last step and was achieved by careful dispersion of the HRP solution (100 μL of HRP solution 250 units/mL) on the activated gold surface till the entire active area was covered with the solution. The system was left in contact over the night at the refrigerator temperature. Then the enzyme supported micro- and nano-patterns were incorporated in flow microreactors (Fig. 1). Before to use the HRP-microreactor, the bioactive surface was gently washed with PBS solution (100 mM, pH 7.4), in order to eliminate the enzyme excess unspecific attached on the gold surface. Microreactors M_2–M_5 were prepared based on this immobilization approach.

The microreactor active area (gold pattern) was regenerated using an electrochemical (cyclic voltammetry) cleaning procedure [40]. Firstly, the microreactor surface was washed several times with 50 mM KOH solution. Then, it was immersed in electrochemical cell containing 50 mM KOH solution and connected to electrical circuit together with the reference and counter electrodes (Ag/AgCl and Pt, respectively). Cell potential was swept from −200 to −1200 mV (vs. Ag/AgCl) at 50 mV/s scan rate once. Then, the gold surface was rinsed in Milli-Q water and the microreactor was re-used in a new approach of HRP immobilization.

2.5. Evaluation of HRP content and activity on gold patterns

The amount of immobilized HRP was determined based on photometric procedure using bovine serum albumin as a standard [41]. The amount of the immobilized enzyme was calculated as the difference between the amount of the initial enzyme added on the pattern surface and the enzyme amount recovered in the wash-solution after enzyme immobilization. HRP activity was assessed from the catalytic oxidation of pyrogallol with H_2O_2 (0.1 mM pyrogallol and 3 mM H_2O_2) by colorimetric estimation of the oxidized product using a spectrophotometer UV-VIS Varian Carry Bio [42]. The colored reaction product was detected at 420 nm wavelength with an extinction coefficient of pyrogallol of 2670 M^{-1} cm^{-1}. The enzyme activity was calculated considering that one activity unit represents the number of pyrogallol micromoles converted per minute at pH 6 and 25 °C.

2.6. Biocatalytic microreactor

The silicon wafers containing the above HRP-gold patterns in pieces of 10 mm × 6 mm were incorporated in a flow microreactor using the design described by Fig. 1. Then, the microreactor was connected to a peristaltic pump (Gilson Minipuls 3, USA) through PTFE tubing (0.5 mm i.d.) and corresponding fittings (Fig. 1). A mixture of 1 mM phenols and 1 mM H_2O_2 in 100 mM PBS (pH 7.4) was carried out in recycling flow within the catalytic microsystem with a flow rate of 100 μL min^{-1}. The catalytic oxidation of phenols was performed at room temperature for at least 24 h achieving minimum 144 cycles with 1 min residence time per cycle.

Finally, the reaction volume was centrifugated at 4000 rpm for 40 min. The precipitate was washed with water, sucked dry on a filter and analysed by NMR spectroscopy. The supernatant was analysis using HPLC-UV/Vis technique. At the end of the experiment, the microreactor was take out from the system, washed carefully with PBS (100 mM, pH 7.4) and stored in PBS solution at 4 °C. A similar procedure was used for the oxidation/polymerization of hydroquinone, cathecol, β-naphtol, resorcine, o-aminophenol, p-aminophenol, 4-metoxyphenol, 2,6-dinitrophenol and 2,4,6-tris(dimethyl-aminomethyl)-phenol.

3. Results and discussion

3.1. Pattern characterization

Fig. 2a shows SEM images of the gold micropatterns resulted from the chemical vapor deposition. It resulted a continuous gold structure at the border with gold grains inside (with an average size around 30–40 nm). Deposition of gold on nano-patterns occurred with the formation of the same continuous gold structure at the border and, inside, with gold grains with a similar size (Fig. 2b). The supported nano-pattern was 180.5 nm large and was covered by nano-grains.

Micro/nano-patterns characterization has also been performed based on STM measurements. Fig. 3 shows the 2D-STM images collected on the gold nano-grains for both micro- (Fig. 3a) and nano-patterns (Fig. 3b). In a good concordance with the SEM results, these pictures demonstrate the deposition of the gold is leading to a random metal deposition irrespective of the size of the patterns. The thickness of the patterns also varied depending on the quantity of the supported gold and on the size of the pattern. Accordingly, it was larger for micropatterns than for nano-patterns.

3.2. Immobilization of HRP enzyme

The HRP-reactor surfaces obtained with both immobilization approaches were characterized based on spectrophotometric technique. The experimental data showed that although the amount of immobilized protein was higher when the enzyme was simply adsorbed compared to covalent immobilization (35 and 20 ng protein/mm^2, respectively). When the enzyme was deposited as monolayer on the microreactor surface, the immobilized HRP was in the range 0.69–3.56 ng/mm^2. It is known that the HRP molecular dimension is of 6.2 nm × 4.3 nm × 1.2 nm = $L \times l \times w$ [43] while the exposed surface of the microreactor was 993.35×10^3 μm^2. Thus, the enzyme amount immobilized on the gold surface calculated based on the experimental data was higher than the theoretical enzyme amount (according to microreactor disposable

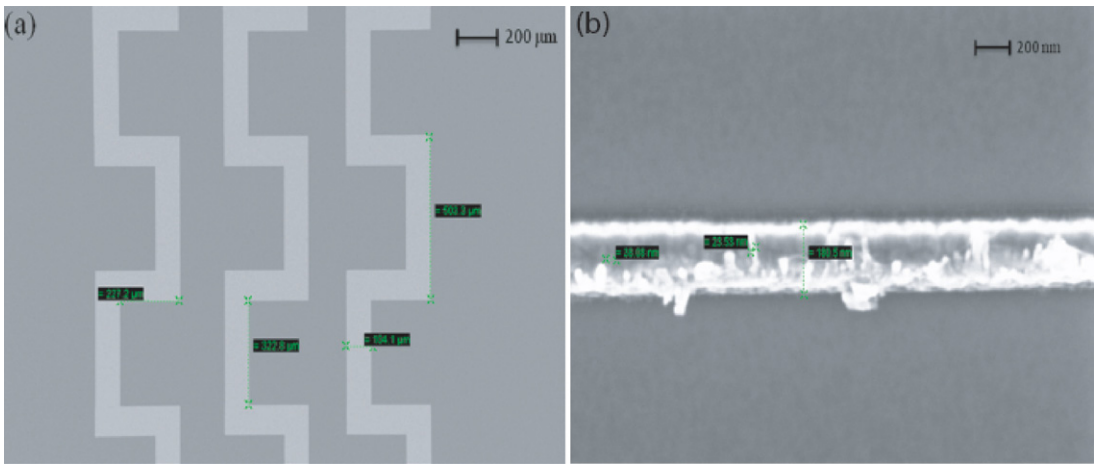

Fig. 2. SEM pictures of gold (a) micro- and (b) nano-patterns.

area). All of those observations have driven to the conclusion that HRP attached enzyme accounts for a multi-layer deposition. This is in line with data previously reported [44]. In addition, the catalytic performances of covalent immobilized enzyme were superior to the attached by adsorption approach (58% and 34% activity yield, respectively) that confirms indeed the model of the multilayer attachment. Based on these observations it was easily to calculate the turnover number (number of phenol molecules converted to product per unit of time) of the enzyme immobilized using different methodologies. Accordingly, it was of $1.96 \times 10^6\ s^{-1}$ and $3.00 \times 10^6\ s^{-1}$ for adsorption and covalent method, respectively, that provides a more clear way to express the efficiency of two methods. The difference can also be explained by the fact that the covalent immobilization *via* self-assembled monolayer (SAM) allows a better orientation of the enzyme on the microreactor surface, while simple adsorption led to the agglomeration of enzyme that may cause a blocking of the active sites. However, the enzyme activity was substantially decreased in both cases.

The bioactive surface of the M_1 and M_2 microreactors has also been investigated using AFM coupled with ellipsometry technique (Fig. 4(a) and (b)). The attached images (Fig. 4) show cross-sections in AFM on a 500 nm × 500 nm scale. Barring the occurrence of aggregates, full coverage of gold of the films is observed, and the cross-sections indicate the size of the structures present on the surfaces (proteins without and with 11-MUA thiol-layer for Fig. 4a and b, respectively). Noticeably, the films without the thiol-layer (i.e. protein adsorption Fig. 4a) exhibit a smaller height than those prepared with pre-incubation of the thiol-layer (covalent attachment of protein Fig. 4b), but in agreement with the size of the proteins (ca. 3 nm). Large aggregates are present on the surface (as high as 60 nm) that appears to be completely covered (no bare gold observed). Thus, both immobilization approaches led to a low homogeneity of the immobilized HRP layer since protein aggregates occurred. However, in agreement to spectrophotometric data, the enzyme distribution seems to be more uniform for covalent attachment than using the adsorption method [45].

Anchoring 11-MUA thiol on the gold patterns made difficult STM identification of the surface gold atoms confirming a quite uniform deposition of these molecules. Further deposition of the HRP enzyme, made even more difficult the identification of the gold layer that represent an additional confirmation of a high coverage.

3.3. HRP-microreactor performance for phenols oxidation

The microreactors performance has been investigated in the HRP oxidation of phenols. As it was mentioned above in the presence of the HRP enzyme the phenols suffer a oxipolymerization leading to polymers with different molecular masses that are insoluble in aqueous medium [46,47]. They precipitate and can easily be removed from the treated water body. ^{13}C NMR spectra of the resulted products confirmed such a behavior (Fig. 5).

The evolution of the oxidative process has been followed based on the phenol conversion. The substrate diffusion under the optimized continue-flow conditions (e.g. flow rate of the reaction phase and reaction time) had no influence on the oxidation process. The use of a non-porous support resulted to be advantageous comparing with porous materials [44,48–50]. Also, minimized diffusion effect is the pattern of the microfluidic device usually [35,51,52]. Thus, the rate of the oxidation process and default the HRP catalytic activity can be attributed to the restricted multi-layer HRP bioactive arrangement instead of diffusion limitation. However, the consumption of H_2O_2 does not directly indicate the efficiency of the oxidation reaction, since H_2O_2 is decomposed at room temperature even in the absence of phenol. Thus, only 12.2% H_2O_2 has been recovered when 1 mM H_2O_2 solution has been left at room temperature for 24 h.

The evaluation of the phenol oxidation in the microreactors showed different performances depending on both the gold

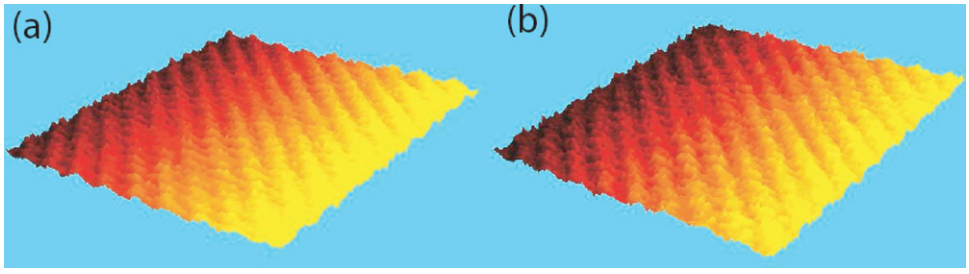

Fig. 3. 2D STM (scanning tunneling microscopy) images of the gold nanograins in (a) micro- and (b) nano-patterns.

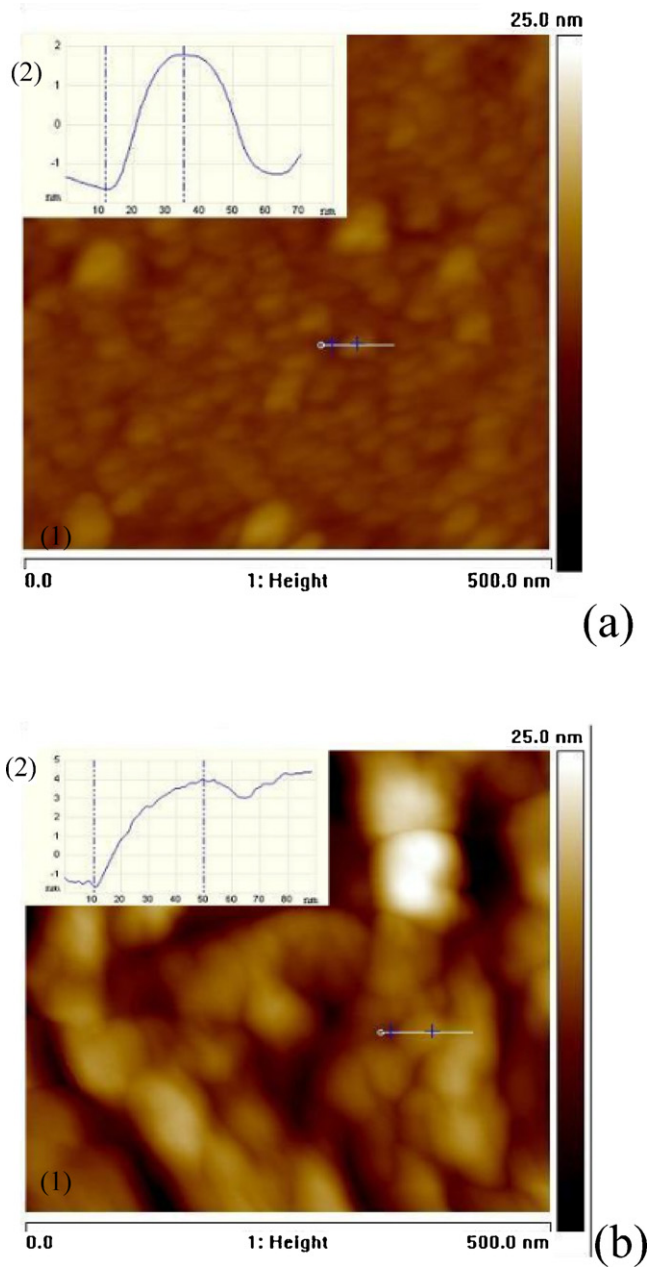

Fig. 4. Characterization of HRP (horseradish peroxidase) – microreactor surface based on AFM (atomic force microscopy) technique (1- cross-section in AFM) coupled with ellipsometry technique (2). (a) HRP immobilized via simple adsorption and (b) HRP covalent immobilized via self-assembled monolayer.

loading and the procedure through which the enzyme has been immobilized. Thus, although M_1 and M_2 had the same gold content and the same area exposed to HRP immobilization (993.35×10^3 μm^2, see Table 1), the oxidation of phenols in these microreactors led to different conversions. The conversion of phenol was lower in the case of physical adsorption than for covalent immobilization (5.2% vs. 7.6% phenol conversion for M_1 and M_2, respectively (Table 1)). These differences may support previous results reported in the literature showing the deposition of enzymes on preorganized self-assembled monolayers provides a better confinement of enzyme and preserves the activity comparing to adsorption approach [53–56]. According to these studies, the physical adsorption to link HRP molecule to a metal surface is not an adequate strategy to generate a bioactive surface. Obviously it induces a weak surface modification that generates conformational

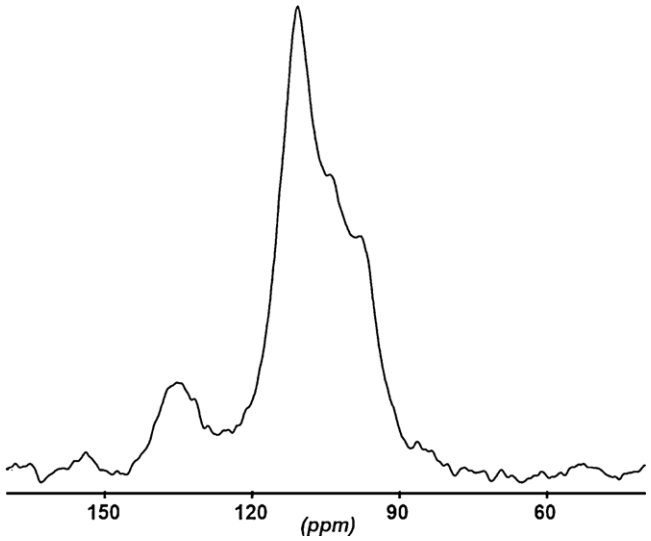

Fig. 5. ^{13}C-CP/MAS NMR spectra of poliphenols.

Table 1
Characterization of the HRP microreactors (the measurements were performed in triplicates $n = 3$).

Microreactor	Thickness of gold pattern (nm)	Gold pattern area[a] (10^3 μm^2)	HRP immobilization approach	Phenol conversion (%)
M_1	217	993.35	Adsorption	5.20 ± 0.17
M_2	217	993.35	SAM	7.60 ± 0.59
M_3	150	1313.29	SAM	9.20 ± 1.05
M_4	130	1470.45	SAM	11.10 ± 1.12
M_5	98	1415.22	SAM	11.30 ± 1.02

SAM – self-assembled monolayer.
[a] The area of gold pattern exposed to HRP immobilization.

changes, denaturation of protein and uncontrolled packing density of the immobilized molecules leading to a steric congestion and also an incompatibility of the substrate to reach the enzyme active sites [56]. In opposite, the self-assembled monolayer approach prevents this kind of incompatibility providing reproducible and reliable platform to immobilized enzyme molecule with required orientation and packing density leading to a better preservation of the enzyme catalytic activity [54].

Under the investigated conditions, the conversion of phenol using the microreactor M_4 was higher as compared with the microreactors M_2 and M_3 prepared in similar way (i.e. HRP covalent immobilization) (7.6, 9.2 and 11.1% phenol conversion for M_2, M_3 and M_4, respectively, see Table 1). This behavior might be assigned to the larger gold area of the M_4 microreactor exposed to HRP attachment (993.35×10^3, 1313.29×10^3, 1470×10^3 μm^2 immobilization area for M_2, M_3 and M_4, respectively, see Table 1). It is important to note that this corresponds to the lowest gold pattern thickness (the same gold amount was deposited onto the micropattern for all of the microreactors) (Table 1).

Noteworthy, a similar phenol conversion to that measured using M_4 has been obtained with the M_5 microreactor (i.e., 11.1% and 11.3% phenol conversion, respectively, Table 1). It must be specified that the M_4 microreactor incorporates a micro-gold pattern, while M_5 microreactor a nano-gold pattern. The enzyme deposition followed the same methodology in both cases. These results confirm the fact the extended surface/loading ratio exposed by the nanopattern is leading to a higher active pattern surface and hence to a better efficiency. It results that the pattern nano-dimension allows a better exposure of the enzyme active sites after immobilization.

To check the endurance of enzyme in these reactors, the HRP-microreactor M_2 was tested in successive cycles (e.g. cycle I, II, III,

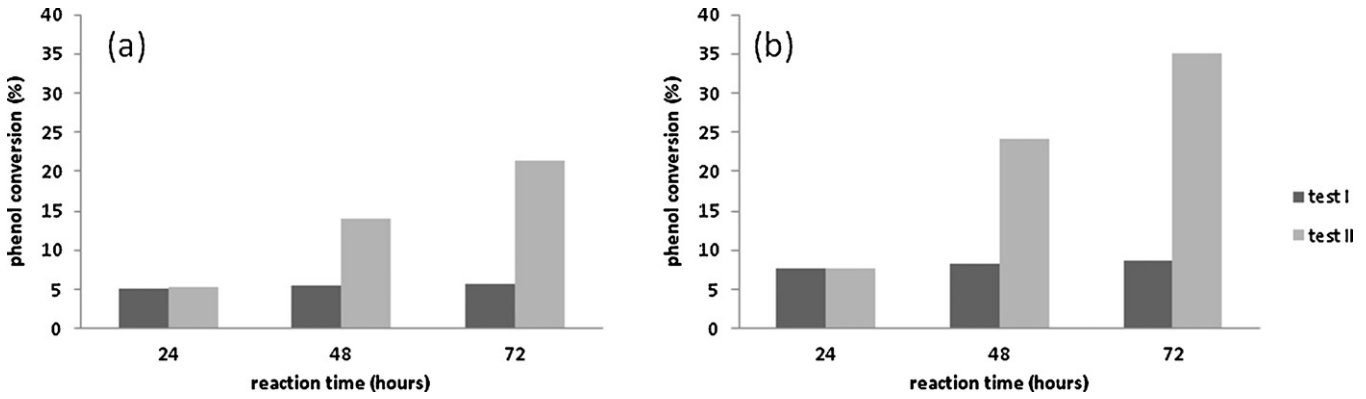

Fig. 6. Improving the phenol conversion by refreshing the H_2O_2 content of the reaction mixture. The experiments (test I and II) have been performed using (a) M_1 and (b) M_2 microreactors. Conditions: initial reaction mixture of 1 mM phenol and 1 mM H_2O_2 solution in 100 mM PBS (pH 7.4), temperature of 25 °C, reaction time of 72 h, and no H_2O_2 addition during the reaction time and 5 μL solution of 1 M H_2O_2 added two times after each 24 h of reaction for test I and II, respectively.

etc.) looking for preservation of the enzyme activity in this reaction. Noteworthy after the first two cycles the conversion was identical (7.6 and 7.7% for cycle I and II, respectively). Only after the third cycle a depletion of the activity with 15% (5.7% conversion for cycle III) has been observed. This could be explained based on HRP inhibition caused by H_2O_2 and phenoxy radicals action. Then, the microreactor surface was electrochemically regenerated and re-used for another HRP immobilization step with good reproducibility according to biocatalytic performances of the bioreactor (5.3% RSD of phenol conversion calculated for $n = 3$). This is a good evidence of the fact that this enzyme can be immobilized in such microreactors and can be reused without a dramatic lose of the catalytic activity at least for several cycles. This behavior is also related to the manner in which the enzyme has been deposited.

The oxidation of phenols in the M_1 and M_2 HRP-microreactors has also been tested in two additional tests: I, in which the reaction mixture of 1 mM phenol and 1 mM H_2O_2 (initial concentrations) was re-cycled through the reactor for 72 h, and II, in which the H_2O_2 content of the reaction mixture was refreshed after each 24 h by adding 5 μL of 1 M H_2O_2 solution in the reaction flow; following this procedure two H_2O_2 additions were performed over the reaction time (72 h). The experimental results were plotted in Fig. 6(a and b) showing interesting conclusions.

In the test I, for the concentration has been used, the phenol consumption was almost completed after 24 h. The prolongation of the reaction time was not accompanied by an increase of the phenol conversion neither after 48 h nor after 72 h, surprisingly. However, an increased phenol conversion was determined after refreshing H_2O_2 content of the reaction phase. Thus, following this procedure the total phenol conversion increased comparing with the test I from 5.6 to 21.4% for M_1 microreactor, and 8.7–35.1% for M_2 microreactor (Fig. 6a and b, respectively). All of the measurements were performed in triplicated with relative standard deviation value corresponding to the range of 3.57–15.91%.

From the practical point of view the use of the microreactor approach is leading to a greater extent of phenol oxidation comparing with that can be achieved under batch conditions (i.e., 11 and 20% conversion under batch system conditions for reactors prepared using adsorption and covalent approach, respectively). Such a conclusion is also valid for the case of M_1 microreactor where the immobilization of enzyme is less effective. More probably this approach avoids the accumulation of the inhibitor products on the HRP-enzyme.

These biocatalytic systems were also tested for the oxidation of several other phenolic compounds, such as hydroquinone, cathecol, β-naphtol, resorcine, o-aminophenol, p-aminophenol, 4-metoxyphenol, 2,6-dinitrophenol and 2,4,6-tris(dimethyl-aminomethyl)-phenol. Except catechol, 4-metoxyphenol, 2,6-dinitrophenol and 2,4,6-tris(dimethyl-aminomethyl)-phenol the conversions were very similar to that of phenol (Table 2) demonstrating the system flexibility for applying to phenol compounds class. The system versatility could be explained based on the selectivity of the HRP enzyme for phenol and phenolic derivatives monosubstituted with hydroxyl and amino group in orto/para position. Polymerization products have been obtained only for hydroquinone, cathecol, β-naphtol and o/p-aminophenol.

Table 2
HRP-catalytic oxidation of phenolic compounds (the measurements were performed in triplicates $n = 3$).

Phenolic compound	Conversion (%)
Phenol	7.60 ± 0.59
Hydroquinone	7.52 ± 1.05
Cathecol	2.36 ± 0.47
Rezorcine	7.54 ± 0.23
β-Naphtol	7.49 ± 1.09
o-Aminophenol	7.03 ± 0.55
p-Aminophenol	6.85 ± 1.11
4-Metoxyphenol	4.03 ± 0.22
2,6-Dinitrophenol	0
2,4,6-Tris(dimethyl-aminomethyl)-phenol	0

4. Conclusion

Intrinsically there are no differences between micro- and nano-lithographic gold patterns versus the immobilization of the HRP-enzyme. Using nano-patterns allows the immobilization of higher loadings of enzyme for a smaller amount of gold that increases the efficiency of the immobilized self-assembled monolayer for the biooxidation of phenols. The HRP-microreactor performances are the consequence of the design and composition of the microreactor pattern (i.e., down scale of the gold pattern dimensions at micro-/nano-level and preserved catalytic activity of the immobilized HRP on the pattern surface). The immobilized enzymes maintained active for several reaction cycles just by intermediate washing with PBS. These experiments confirmed that the immobilization of the enzyme allows the biocatalyst to survive longer under the process conditions, making the biocatalyst reusable. Another advantage of the system is the fact the microreactor active area can be easily regenerated using an electrochemical cleaning procedure that allows the re-use of microreactor with similar performances for enzyme immobilization. Furthermore, the performances of the developed biocatalytic system allow considering its extension as lab on chip device to biosensor field as future perspective.

Acknowledgments

The authors acknowledge the partial funding by EU FP6 program contract RITA-CT-2003-506095 and by CNCSIS-UEFISCU, project number PN II-IDEI 548/2008 and PN II-UMANE RESURSE TE 91/2010.

References

[1] R. Huszank, S.Z. Szilasi, K. Vad, I. Rajta, Nucl. Instrum Methods Phys. Res. Section B: Beam Interact. Mater. Atoms 267 (2009) 2299–2301.
[2] P.L. Mills, D.J. Quiram, J.F. Ryley, Chem. Eng. Sci. 62 (2007) 6992–7010.
[3] J.J. Lerou, A.L. Tonkovich, L. Silva, S. Perry, J. McDaniel, Chem. Eng. Sci. 65 (2010) 380–385.
[4] A. Green, B. Johnson, A. John, Chem. Eng. 106 (1999) 66–76.
[5] D.C. Hendershot, Chem. Eng. Prog. (2000) 35–40.
[6] A.I. Stankiewicz, J.A. Moulijn, Chem. Eng. Prog. (2000) 22–34.
[7] H. Uvet, T. Arai, Y. Mae, T. Takubo, M. Yamada, Adv. Robotics 22 (2008) 1207–1222.
[8] K.F. Jensen, Ernst Schering Foundation Symposium Proceedings, 2006, pp. 57–76.
[9] Y. Wu, K.E. Taylor, N. Biswas, J.K. Bewtra, J. Environ. Eng. 125 (1999) 451–458.
[10] L.F. Liotta, M. Gruttadauri, G. Di Carlo, G. Perrini, V. Librando, Hazard. Mater. 162 (2009) 588–606.
[11] K. Hamamoto, H. Kawakita, K. Ohto, K. Inoue, Reactive Funct. Polym. 69 (2009) 694–697.
[12] I. Alemzadeh, S. Nejati, J. Hazard. Mater. 166 (2009) 1082–1086.
[13] F.-Y. Jeng, S.-C. Lin, Process Biochem. 41 (2006) 1566–1573.
[14] D.S. Kobayashi, RitterF H., D. Kaplan, in: D.S. Kobayashi, H. Ritter, D. Kaplan (Eds.), Advances in Polymer Science, Springer, Berlin, 2006.
[15] M. Reihmann, H. Ritter, Adv. Polym. Sci. 194 (2006) 1–49.
[16] R.A. Gross, A. Kumar, B. Kalra, Chem. Rev. 101 (2001) 2097–2124.
[17] N. Duran, E. Esposito, Appl. Catal. B: Environ. 28 (2000) 83–99.
[18] S. Akhtar, Q. Husain, Chemosphere 65 (2006) 1228–1235.
[19] W. Tischer, V. Kasche, Trends Biotechnol. 17 (1999) 325–336.
[20] J.L. Gómez, A. Bódalo, E. Gómez, J. Bastida, A.M. Hidalgo, M. Gómez, Enzyme Microb. Technol. 39 (2006) 1016–1022.
[21] K.F. Fernandes, C.S. Lima, F.M. Lopes, C.H. Collins, Process Biochem. 39 (2004) 883–888.
[22] P. Peralta-Zamora, E. Esposito, R. Pellegrini, R. Groto, J. Reyes, N. Duran, Environ. Technol. 19 (1998) 55–63.
[23] S. Dalal, M.N. Gupta, Chemosphere 67 (2007) 741–747.
[24] S. Yuan, R. Yuan, Y. Chai, Y. Zhuo, X. Yang, Y. Yuan, Appl. Biochem. Biotechnol. (2010) 2010, published online on June.
[25] Y. Wang, X. Ma, Y. Wen, Y. Xing, Z. Zhang, H. Yang, Biosens. Bioelectron. 25 (2010) 2442–2446.
[26] L. Pramparo, F. TStuber, J. Font, A. Fortuny, A. Fabregat, C. Bengoa, J. Hazard. Mater. 177 (2010) 990–1000.
[27] P.R.S. Leirião, L.J.P. Fonseca, M.A. Taipa, J.M.S. Cabral, M. Mateus, Appl. Biochem. Biotechnol.: Part A Enzyme Eng. Biotechnol. 110 (2003) 1–10.
[28] K.F. Fernandes, C.S. Lima, H. Pinho, C.H. Collins, Process Biochem. 38 (2003) 1379–1384.
[29] V. Vojinovic, R.H. Carvalho, F. Lemos, J.M.S. Cabral, L.P. Fonseca, B.S. Ferreira, Biochem. Eng. J. 35 (2007) 126–135.
[30] G.A. Messina, A.A.J. Torriero, I.E.D. Vito, J. Raba, Talanta 64 (2004) 1009–1017.
[31] A.M. Azevedo, V. Vojinovic, J.M.S. Cabral, T.D. Gibson, L.P. Fonseca, J. Mol. Catal. B: Enzym. 28 (2004) 121–128.
[32] J.A. Nicell, J.K. Bewtra, N. Biswas, E. Taylor, Water Res. 27 (1993) 1629–1639.
[33] A. Pintar, J. Levec, J. Catal. 135 (1992) 345–357.
[34] A. Pintar, J. Levec, Ind. Eng. Chem. Rev 33 (1994) 3070–3077.
[35] P. Fernandes, Int. J. Mol. Sci. 11 (2010) 858–879.
[36] E.M. Alhadeff, A.M. Salgado, N. Pereira Jr., B. Valdman, Appl. Biochem. Biotechnol.: Part A Enzyme Eng. Biotechnol. 121 (2005) 361–371.
[37] X.M. Jiang, Z.C. Chen, S.M. Yang, H.F. Lin, X.F. Lin, Chin. Chem. Lett. 15 (2004) 547–550.
[38] A. Srinivasan, X. Wu, M.-Y. Lee, J.S. Dordick, Biotechnol. Bioeng. 81 (2003) 563–569.
[39] D. Massiot, F. Fayon, M. Capron, I. King, S.L. Calve, B. Alonso, J.-O. Durand, B. Bujoli, Z. Gan, G. Hoatson, Magn. Reson. Chem. 40 (2002) 70.
[40] L.M. Fischer, M. Tenje, A.R. Heiskanen, N. Masuda, J. Castillo, A. Bentien, J. Émneus, M.H. Jakobsen, A. Boisen, Microelectronic Engineering MNE'08—the 34th International Conference on Micro- and Nano-Engineering (MNE), 86, 2009, pp. 1282–1285.
[41] E.F. Hartree, Anal. Biochem. 42 (1972) 422–427.
[42] B. Halpin, R. Pressey, J. Jen, N. Mony, J. Food Sci. 54 (1989) 644.
[43] J.D. Zhang, Q.J. Chi, S.J. Dong, E.K. Wang, Bioelectrochem. Bioeng. 39 (1996) 267–274.
[44] I. Magario, X. Ma, A. Neumann, C. Syldatk, R. Hausmann, J. Biotechnol. 134 (2008) 72–78.
[45] F. Vianello, L. Zannaro, M.L. di Paolo, A. Rigo, C. Malacarne, M. Scarpa, Biotechnol. Bioeng. 68 (2000) 488–495.
[46] Z. Huixian, K.E. Taylor, Chemosphere 28 (1994) 1807–1817.
[47] L.S. Andrade, E.A. Laurindo, R.V. de Oliveira, R.C. Rocha-Filho, Q.B. Cass, J. Braz. Chem. Soc. 17 (2006) 369–373.
[48] D.D. Lee, G.K. Lee, P.J. Reilly, Y.Y. Lee, Biotechnol. Bioeng. 22 (1980) 1–17.
[49] R.J. Baross, E. Wehtje, P. Adlercreutz, Biotechnol. Bioeng. 67 (2000) 319–326.
[50] R.J. Baross, E. Wehtje, F.A.P. Garcia, P. Adlercreutz, Biocatal. Biotransform. 16 (1998) 67–85.
[51] M. Miyazaki, H. Maeda, Trends Biotechnol. 24 (2006) 463–470.
[52] R.L. Hartman, K.F. Jensen, Lab Chip 9 (2009) 2495–2507.
[53] R.K. Mendes, R.F. Carvalhal, L.T. Kubota, J. Electroanal. Chem. 612 (2008) 164–172.
[54] F. Wu, Z. Hu, J. Xu, Y. Tian, L. Wang, Y. Xian, L. Jin, Electrochim. Acta 53 (2008) 8238–8244.
[55] N.K. Chaki, K. Vijayamohanan, Biosens. Bioelectron. 17 (2002) 1–12.
[56] L.S. Wong, F. Khan, J. Micklefield, Chem. Rev. 109 (2009) 4025–4053.